Analysis of Bearing Damage Using a Multibody Model and a Test Rig for Validation Purposes

W. JACOBS, M. MALAGÓ, R. BOONEN, D. MOENS and P. SAS

ABSTRACT

Intensive research, performed over the last five decades, focuses on fault diagnosis of bearings. To investigate the generation of these fault symptoms, this paper discusses the development of a multibody model of a bearing. Localized faults are introduced in the model, aiming to analyse vibration signals of damaged bearings. The paper compares different possibilities to implement these defects. Simultaneously, a test rig is built to validate the model. The rig allows applying a fully controlled multi-axial static and dynamic load on different types of bearings. Therefore, it is a powerful tool to load a bearing as built into a real machine, and measure its response.

INTRODUCTION

Bearings are one of the most used components in mechanical machines. However, they are also one of the most critical components, and bearing failure can have serious economical consequences. Therefore, intensive research, performed over the last five decades, focuses on fault diagnosis of bearings and bearing modelling [1]. A study conducted at the K.U.Leuven investigates the effects of typical mechanical bearing faults based on a multibody model of a bearing. In a first step, a multibody model of a bearing is built, and a multi-purpose test rig is developed to validate the models of healthy and damaged bearings. In this way, the study aims to gain insight into diagnostic signals of faulty bearings, leading to improved condition monitoring techniques.

The first part of this paper presents the development of a multibody model of a bearing, and the introduction of faults into this model. The implementation of faults in a bearing model will give a better understanding of the generation of fault symptoms, in particular where non-linear interactions are involved [2]. Fault simulation can also be very valuable to produce signals with well-defined characteristics, for example to train neural networks for diagnostics and prognostics of a range of different fault types and locations in machines [3].

William Jacobs, Department of Mechanical Engineering, K.U.Leuven, Celestijnenlaan 300B, B-3001 Heverlee, Belgium, e-mail: William.Jacobs@mech.kuleuven.be
Marco Malagó, Universitá degli studi di Ferrara, Via Saragat 1, I-44100 Ferrara, Italy, e-mail: Marco.Malago@unife.it

After a brief overview of the work done in the bearing modelling domain, the paper describes how the model is built and how the contact between the different bodies, based on the Hertz theory, is implemented. Furthermore, the possibility to add localized spalls on the surface of the raceways is being investigated. To define the contact between spalled surfaces, it was concluded that a different contact algorithm should be used.

The second part of the paper focuses on the design of a test rig, to apply a fully controlled load on a bearing and measure its response. The rig is not only an effective tool to validate multibody models. It can also be used to test condition monitoring techniques for bearings, free from disturbances occurring from other components existing in a real machine. The test rig innovates in two ways. Firstly, different types of bearings, such as deep groove ball bearings and tapered roller bearings, and different sizes of bearings can be mounted. In this way, the rig can be used to validate models of different bearings. The design allows easy adjustment of the test rig to mount bearings with different inner diameter, outer diameter and width, without compromising on performance. Secondly, the applied load on the bearing is multi-axial, with a component in the radial and axial direction of the bearing, and is both static and a dynamic in each direction. Thereby, it is possible to load the bearing as if it were built into a real machine, for example a gearbox.

The aim to apply a dynamic force on the bearing complicates the design considerable. High requirements are imposed on the dynamic behaviour of the vibrating parts of the set-up. In the last part of the paper, this is discussed in detail.

BEARING MODELLING

The first bearing simulation models aimed to describe the influence of the physical characteristics and operational conditions through an analytical approach. The first rolling element bearing models were built by Lundberg and Palmgren [4], assuming non-linear stiffness and time-invariance. Akturk [5] and Gupta [6] investigated the complete field of the non-linear and time-varying characteristics, relating the main causes of non-linearity to the Hertzian force and deformation factors, the compliance effect, the clearance between the rolling elements and the rings and the effect of the lubrication. Tiwari [7] analysed the effect of ball bearing clearance on the dynamic response of a rigid rotor. Elasto-hydrodynamic lubrication (EHL) was added to the models by Wijnat [8], discovering that the effect of the EHL is moderate for medium loads and low rotational speeds. Most recently, Sopanen and Mikkola [9] developed different models taking into account the non-linear and time-varying characteristics, the EHL and the effect of localized defects on the surface of the inner and outer ring of the bearing.

Multibody model description and assumptions

A deep groove single row ball bearing 6302 is modelled as a multibody system using the commercial software LMS Virtual.Lab Motion. The bearing model is composed of different bodies with a well known geometry, namely the inner and outer ring, seven rolling elements and the shaft, as shown in Fig. 1.

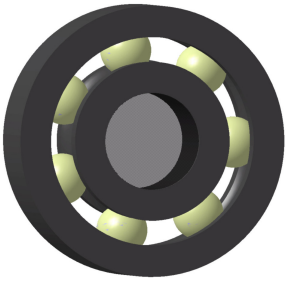

Figure 1. Multibody model of a bearing

The different bodies are considered rigid, in order to obtain detailed information about their dynamic behaviour at low and medium frequencies. This assumption however limits the correctness of the observations at high frequencies. Therefore, in the future the model will be improved by considering these bodies flexible. Furthermore, the following assumptions are made:

- the contact stiffness between the rings and rolling elements is fully determined using the non-linear Hertzian contact deformation theory;
- the outer and inner ring, the rolling elements and the shaft are rigid. Only local deformation in the contact area occurs;
- the cage is assumed to be ideal, maintaining a fixed relative distance between the rolling elements;
- the centrifugal force acting on the rolling elements is negligible;
- the damping caused by the EHL is negligible for the simulations at relatively low speed.

The non-linear Hertzian contact deformation algorithm, elliptical contact conjunction (ECC) [10], is adopted in the model to define the contact between each rolling element and the inner and outer ring. This contact tool allows representing the contact and friction forces of the elements rolling around the raceways. It uses the following inputs: the geometry, the friction coefficient, the material properties and the damping coefficient. It then gives the following outputs: the displacements, velocities and accelerations of the different components and the resulting forces and torque.

Introduction of damage

To investigate the influence of damage on the behaviour of a bearing, a local spall is introduced on the outer ring of the model. However, due to the presence of localized discontinuities, the model no longer meets the main Hertzian assumptions. The ECC algorithm is therefore unable to represent the real force between the rolling element and the raceway in case of localized defects. In particular, when the centre of the rolling element enters the defect, the force between the two bodies becomes zero and returns to the original values only when the rolling element centre leaves the defect. Fig. 2 compares the real and the simulated trajectory of the rolling element.

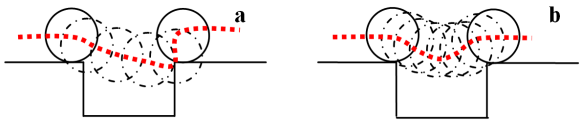

Figure 2. Simulated (left) and real (right) trajectory of a rolling element through a spall

To overcome this limitation, a different algorithm, the polygonal contact model (PCM), is used to define the contact [11, 12]. This technique is based on the representation of the body surfaces by polygon meshes. The contact is examined after discretizing the contact patch. This can be regarded as a compromise between the simple ECC contact approach and the costly FEA. It is better suited to represent localized physical phenomena then ECC, with lower computation time compared to FEA. The PCM task consists of three steps. First, a collision detection algorithm determines if the contact pair is in touch. If no collision is detected, the program returns zero force and torque and the analysis is finished. Otherwise, PCM constructs the intersecting areas of the surfaces and discretizes the corresponding contact patches in the second step. Finally, for each element the contact force is determined, and the resulting total contact force and torque is calculated.

Due to the low computation efficiency of the PCM, the algorithm was tested using a simplified model. Three rolling elements, separated using two distance constraints, are guided by a faulty lower surface and an upper healthy surface, as shown in Fig. 3. A macro-defect of 1.3 mm and a rolling element radius of 6 mm are considered. The simplified model is used to analyse the advantages and disadvantages of both techniques. The PCM algorithm is characterized by the following properties:

- the contact is examined using a discretization of the contact patch;
- the algorithm provides the possibility to measure the contact between the rolling elements and localized raceway faults;
- the computation time of the algorithm is high.

On the contrary, in the ECC algorithm:

- the rigid contact bodies are not discretized;
- the contact force is based on the non-linear Hertzian theory;
- the computation time is small.

Despite the fact the ECC algorithm is unable to accurately simulate vibration signals of spalled structures, it can be considered as a powerful and efficient tool to model healthy and damaged bearings. Fault signals can be analysed in frequency domain, as the characteristic defect frequencies only depend on the impulse periodicity of the impacts, not the rolling element trajectory.

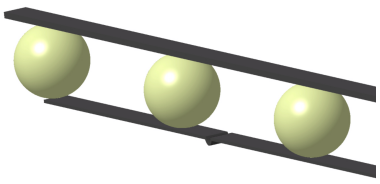

Figure 3. Simplified model of a rolling element passing a spall

BEARING TEST RIG

In literature, many different designs of bearing test rigs have been proposed. Most of these set-ups are able to apply a static load on a bearing, using for example hydraulics or springs. Some excite the bearing in its radial direction, some in its axial direction and some in both directions. Bearing manufactures even offer these types of test rigs, allowing the costumers to test the quality of the grease they are using. Other types of test rigs load the bearing using an unbalance weight on a shaft, or through a set of gears using a gearbox [3]. The latter rigs can be used to validate techniques developed to detect bearing damage in signals dominated by gear meshing noise. For the sake of completeness, the four-ball [13] and five-ball [14] rolling contact fatigue test rigs are mentioned here as well. These rigs are commonly used to investigate friction and surface wear in the contact area. Only one rolling element of the bearing is being examined. The results are afterwards extended to the system level of an entire bearing.

Although many research projects conducted in the past use bearing test rigs, none of the rigs are able to apply a fully controlled multi-axial static and dynamic load on the bearing. Therefore, a new type of test rig was developed in the framework of the study.

Test rig design

The main principle of this test rig is fairly simple. A radial and axial load is applied on a test bearing, which is mounted on a shaft and driven by an electric motor. To counteract the load, two other bearings support the shaft. The load is directly applied on the stationary outer ring of the test bearing. Fig. 4 shows the concept and an overview of the test rig.

The rig should make it possible to test bearings of different types, such as deep groove ball bearings, angular contact ball bearings and tapered roller bearings, and bearings of different sizes, with an inner bore diameter varying from 10 to 19 mm, an outer diameter varying from 20 to 52 mm and a width varying from 5 to 15 mm. Therefore, it should be possible to adjust the shaft to different inner bore diameters of the test bearing. This is realised using a clamping mechanism called collet chuck. In milling machines, a collet chuck is used to clamp the tool into the main spindle. The test bearing is mounted on a small auxiliary shaft, adapted to its bore diameter.

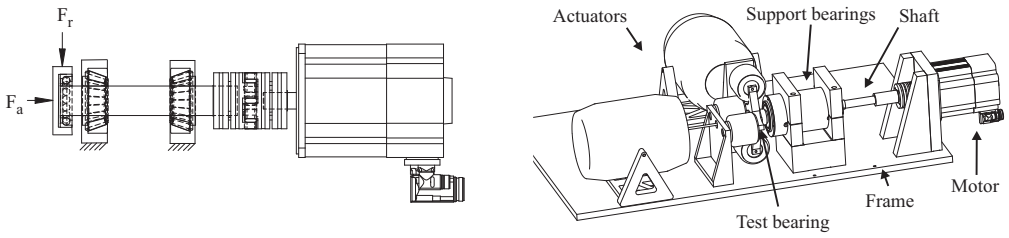

Figure 4. Concept (left) and overview (right) of the test rig

After inserting this auxiliary shaft, the locknut is tightened forming a stiff connection between the main shaft and the auxiliary shaft. Furthermore, both shafts are perfectly aligned, due to the tapered shape of the mating parts. On the other hand, the housing of the test bearing should be adjusted to a different width and different outer diameter. This is possible by mounting the bearing in an intermediate adaptor sleeve, between the bearing and the housing. The bore diameter of this sleeve is adapted to the outer diameter of the test bearing.

The load imposed on the bearing should be controlled in the radial and axial direction, independent of each other. No coupling between the radial and axial force is therefore allowed. Furthermore, the load should have a static and dynamic component in both directions. No coupling between the static and dynamic force is allowed. In this way, it will be possible to simulate different real-life situations, where i.e. gear meshing forces are acting on the bearing. Both static and dynamic components are provided by a different type of actuator. Air springs are used to apply a static force up to 10 kN in each direction. The air springs consist of two parallel plastic disks, connected through a rubber sleeve. Pressurized air in this sleeve provides the static force. The force will be controlled by pressure regulators in the air circuit. The dynamic actuators should provide a broadband dynamic force from 10 to 500 Hz. Electrodynamic shakers are used to generate this force. After defining the different actuators, they are positioned around the test bearing. Fig. 5 gives an overview of the actuator configuration. In the right part, the actuators are replaced by force vectors, providing a clear view on the design of the bearing housing. The static load is generated by four air springs, transferring their force to the bearing using an arm on the housing. Two air springs control the axial force ($F_{a,st}$) and two air springs control the radial force ($F_{r,st}$). The dynamic load is directly introduced on the bearing housing through the stingers of the shakers: one stinger for the axial direction ($F_{a,d}$) and one stinger for the radial direction ($F_{r,d}$).

The test bearing is instrumented with sensors commonly used for condition monitoring of bearings. Four accelerometers are mounted on the housing, as close as possible to the bearing itself. Three capacitive proximity probes measure the relative displacement between the inner and outer ring of the bearing. Two of these probes measure the full radial motion of the inner ring, as they are positioned perpendicular to each other. One probe measures the axial motion of the inner ring. One thermocouple is mounted in the seat of the bearing and measures the outer ring temperature.

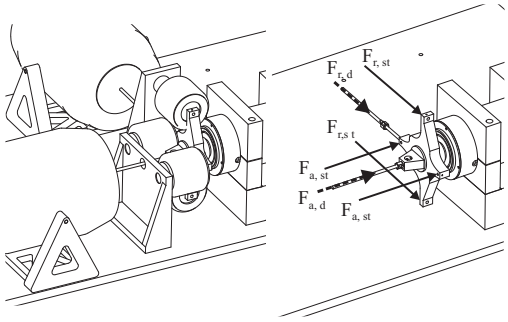

Figure 5. Actuators (left) and their corresponding force vectors (right)

Dynamic analysis of the test rig

Applying a dynamic force on the bearing complicates the design of the test rig considerable. To evaluate the ability of the housing to transfer the dynamic forces to the bearing, a dynamic FEM analysis is performed. The ability to transfer the forces depends on the resonances in the structure. If a resonance occurs in the frequency range of excitation, the structure acts as a filter blocking the excitations above this resonance. Therefore, the first resonance of the housing should occur sufficiently above the maximum excitation frequency. More precisely, the first resonance should be located above $500\sqrt{2}$ Hz. In the final design, the first mode of the housing occurs at a resonance frequency of 1143 Hz.

When analysing a bearing using the test rig, the measurements should not be influenced by the dynamics of the rig. Recalling that the test bearing is excited in a range from 10 to 500 Hz, the structure should be resonance free up to $500\sqrt{2}$ Hz. The design of the frame is adapted to satisfy this condition. The entire test rig is analysed using FEM software. Here, the housing of the test bearing is modelled as a simple point mass. Also, the test bearing is modelled as a spring. This simplification is allowed, as the dynamic behaviour of these parts was already investigated in the previously described analysis. The FEM analysis of the test rig showed a first bending resonance of the frame at 1266 Hz and a first bending of the shaft at 805 Hz. It can consequently be concluded that the system is resonance free in the full excitation range of the shakers.

In Fig. 6, the first bending mode of the housing and the frame is visualised.

CONCLUSIONS

The multibody bearing model presented in this paper is an interesting tool to investigate fault symptoms of damaged bearings. Localized spalls can be introduced on the surface of the raceways, and the response signals of the bearing can be analysed. To validate this model, an innovative and versatile bearing test rig was developed, as discussed in the second part of the paper. The test rig allows easy adjustment to mount different types and sizes of bearings. The bearings can be preloaded up to 10 kN, and excited up to 500 Hz. In this way, a wide range of bearings can be tested in real-life conditions. The aim to apply a dynamic force on the bearing complicates the design considerable. The entire set-up is optimised to keep the components free from resonances in a wide excitation range.

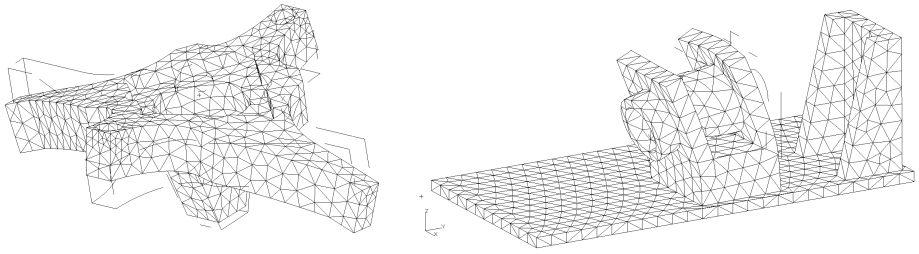

Figure 6. First mode of the housing (left) and the frame (right)

ACKNOWLEDGEMENT

This research is funded by a Ph.D. grant of the Agency for Innovation by Science and Technology (IWT). Part of this work was performed through the support of the IWT SBO-project no.090045 Prognostics for Optimal Maintenance.

REFERENCES

1. Williams, T., Ribadeneria, X., Billington, S., and Kurfess, T. 2001. "Rolling element bearing diagnostics in run-to-failure lifetime testing," *J. of Mechanical Systems and Signal Processing,* 15(5): 979–993.
2. Sawalhi, N., and Randall, R. 2010. "Improved simulations for fault size estimation in rolling element bearings," presented at the Seventh International Conference on Condition Monitoring and Machinery Failure Prevention Technologies, June 22-24, 2010.
3. Sawalhi, N., and Randall, R. 2008. "Simulating gear and bearing interactions in the presence of faults - Part I. The combined gear bearing dynamic model and the simulation of localised bearing faults," *J. of Mechanical Systems and Signal Processing,* 22(8): 1952–1966.
4. Lundberg, G., and Palmgren, G. 1947. "Dynamic capacity of rolling bearings," *Acta Polytechnic Mechanical Engineering Series,* 1(3): 5–50.
5. Akturk, M., Gupta, K., and Gohar, R. 1997. "The effects of number of balls and preload on vibrations associated with ball bearings," *J. of Tribology,* 119: 747–753.
6. Gupta, K. 1988. "On the geometrical imperfections in ball bearings," *J. of Tribology,* 110: 19–25.
7. Tiwari, M., Gupta, K., and Prakash, O. 2000. "Effect of radial internal clearance of ball bearing on the dynamics of a balanced horizontal rotor," *J. of Sound and Vibration,* 238: 723–756.
8. Wijnat, Y., Wensing, J., and Van Nijen, G. 1999. "The influence of lubrication on the dynamic behaviour of ball bearings," *J. of Sound and Vibration,* 222(4): 579–596.
9. Sopanen, J. an Mikkola, A. 2003. "Dynamic model of a deep-groove ball bearing including localized and distributed defects. Part 1: theory," *J. of Multibody-Dynamics,* 217(3): 201–211.
10. Young, W., and Budynas, R. 2002. *Roark's Formula for Stress and Strain.* McGraw Hill.
11. SKF. 2008. *SKF General Catalogue.* SKF Group.
12. Hippmann, G. 2004. "An algorithm for compliant contact between complexly shaped bodies," *J. of Multibody System Dynamics,* 12: 345–362.
13. Rico, J., Battez, A., and Cuervo, D. 2003. "Rolling contact fatigue in lubricated contacts," *J. of Tribology International,* 36(1): 35–40.
14. Zaretsky, E., Parker, R., and Anderson, W. 1982. "NASA five-ball fatigue tester: Over 20 years of research," *ASTM special technical publication,* (771): 5–45.
15. Brändlein J., Eschmann P., H. L., and K., W. 1999. *Ball and Roller Bearings: Theory, Design and Application.* Wiley.
16. Harris, T. A., and Kotzalas, M. N. 2007. *Rolling Bearing Analysis - Essential Concepts of Bearing Technology.* Taylor and Francis Group, Boca Raton.